

Nonlinear Phenomenon in High-Speed Yarn Transport

(Annual Report, March 1., 1994-Present)

Code Number: S94-9

PI(s): Tushar K. Ghosh, Subhash K. Batra, William Oxenham (NCSU)

B. C. Goswami, C. Rahn (Clemson)

W. B. Fraser (University of Sydney, Australia)

Graduate Students: A. Murthy, Q. Zeng (NCSU), R. Nerlagunte, J. Malsam (Clemson)

Research Goals

High-speed movement of yarns to and from packages is common to many textile processes. In cases where the yarn rotates around the axis of a stationary package in the process of unwinding or that of a rotating package in the process of twisting and winding (ring spinning, etc.), the inertial forces tend to create an enveloping surface called the balloon. The shapes of the balloon envelopes and tension distribution are critical to the performance of the processes. In a recently completed project, these processes have been modelled using basic laws of physics and it was revealed that the governing equations of motion are highly nonlinear. To continue evolution of the unified theory and to obtain results of practical consequence, the primary goals of the present research are:

- to develop a unified theory to analyze the nonlinear nature of tension and balloon shape fluctuation in textile processes involving high speed translational and rotational movement of yarns.
- to validate the theoretical observations with suitable experiments.
- to develop computational tools for the analysis and set-up of equipments in manufacturing environment.

Abstract

The shape and tension distribution in yarns in case of over-end unwinding of yarns from stationary cylindrical packages and ring spinning are analyzed.

Yarn motion in over-end unwinding is considered in two stages; (1) from the unwind point to the lift-off point and, (2) from lift-off point to the thread-guide when the yarn is in the balloon. The behavior of unwinding balloon is studied for various values of wind angle, the drag between package and the yarn, and residual tension. It was found that for a given wind angle a family of solutions corresponding to various levels of tension distribution is obtained. On the other hand specification of residual tension as a boundary condition results in unique solutions.

In ring spinning the domains of instability have been mapped. The effect of control rings and related parameters on eliminating the instability are being studied.

Introduction:

Yarns are fundamental to the production of most consumer and industrial textiles. During their manufacture and subsequent use, they are transported from one cylindrical package (bobbins, cones included) to another in order to either improve their quality/performance characteristics (evenness, texture, strength/integrity) or to improve performance of the subsequent processing steps (e.g. warping, weaving). In a number of these situations, the optimal mechanism (high speed and productivity) to accomplish the task is that of over-end winding or unwinding. The levels of optimality in a number of these cases, however, have reached a plateau because use of higher speeds, larger package sizes, coarser (higher mass linear density) yarns lead to unacceptable rates of "ends-down," or yarn breakages. The latter are a result of the dynamic tensions, engendered in the yarn, which exceed "local" strength of the yarn. The cost of yarn breakages to the industry can be very significant if one adds up the material wastage, loss of labor and machine productivity, and influence on quality of the final products. In the research currently underway, fundamental mechanisms that give rise to fluctuating tensions during unwinding of a cylindrical package from start to finish are being studied.

In the same vein, staple fiber (short or long) yarns spun on millions of ring spinning spindles remain dominant part of the US yarn market for carpets, wovens, knits, threads/cords, etc. Indeed, in the short staple system, at least, the recent renaissance in this technology has brought about the concept of individual (hopefully programmable) spindle drives, pushed the spindle speeds up to 25,000 rpm, and with the help of "super drafting" systems made it possible to spin directly from slivers. Despite these dramatic advances, optimal productivity of the corresponding capital intensive machines remains governed by the "ends-down" rate. Experimental investigations in the industry have revealed spinning tension fluctuation range two to three times larger than forecast by the best available models at the start of this research. More accurate/realistic models are needed to bring predictions in harmony with observed

reality. Such models will help bring about productivity gains together with improvements in the cost/quality equation. ~~Even a modest gain in this context will have a disproportionately large impact because of the very large number of spindles in use in the US industry.~~

A significant part of the plied yarn industry (for sewing threads, three or four ply cords, plied carpet yarns, etc.) uses ring twisting for insertion of twist. The mechanism of ring twisters used is very often similar, if not identical, to the ring spinning process. The knowledge gained in the study of ring spinning will be almost directly applicable to the plied yarn industry.

The Mathematical Formulation

The theory of over-end unwinding of yarn from a stationary package and balloon formation in the ring-spinning process have both received considerable attention in the industry and extensive research literature exists in these areas. A comprehensive investigation of the dynamics of over-end unwinding has been reported by Padfield¹ and subsequently Kothari and Leaf² reported extensive numerical calculation based on Padfield's analyses. However, the efforts to understand the underlying generality of these processes and to develop a unified framework to deal with the complex time-dependence of these problems started with the present work. In the following we describe the general mathematical formulation of the problem and then look at specific examples of unwinding, 2-for-1 twisting, and ring spinning. In developing the mathematical formulation, the yarn has been assumed to be inextensible, perfectly flexible and of uniform density and cross-section so that only tension and air drag forces act on the yarn.

Equation of Motion of Yarn in Space

Consider a material point P (Figure 1) on the yarn which at time t is at a distance s measured along the yarn from the guide-eye. Let, $R(s,t) = re_r + zk$, be the position vector of P relative to an origin of a coordinate system positioned at the guide-eye O. Let r, θ , and z be cylindrical coordinates corresponding to unit base vectors e_r, e_θ, k of a coordinate system that rotates with a constant angular velocity ωk about the z axis, which coincides with the axis of the spindle. The direction of the z -axis is positive down towards the yarn package.

If $T(s,t)$ is the tension in the yarn at P then the full vector form of the time dependent equations of motion for the free yarn element at P in terms of non-dimensional parameters is [1,2,3]

$$D^2\bar{R} + 2\Omega k \wedge D\bar{R} + \Omega^2 k \wedge (k \wedge R) = \frac{\partial}{\partial \bar{s}} \left(T \frac{\partial \bar{R}}{\partial \bar{s}} \right) + \bar{F} \quad (1)$$

The differential operator D is given by, $D = \epsilon \frac{\partial}{\partial t} - V \frac{\partial}{\partial s}$

where V is constant linear speed of the thread-line or the yarn, m is the linear density of the yarn, c is radius of the package or the ring, and τ_0 is the period of unwind in case of unwinding, and $\epsilon = \frac{c}{V\tau_0}, \Omega = \frac{\omega c}{V}$

The non-dimensional variables can be defined as:

$$\bar{R} = \frac{R}{c} = \frac{r}{c} e_r + \frac{z}{c} k = \bar{r} e_r + \bar{z} k, \quad \bar{s} = \frac{s}{c}, \quad \bar{t} = \frac{t}{\tau_0}, \quad \bar{v}_n = \frac{v_n}{V}, \quad \bar{v} = \frac{v}{V}, \quad \text{and,} \quad \bar{T} = \frac{T}{mV^2}, \quad \bar{F} = \frac{Fc}{mV^2}, \quad \bar{N} = \frac{Nc}{mV^2}$$

The operator D is the total time derivative following the motion of P relative to the rotating frame. Thus $D\bar{R}$ is the velocity of the material particle P and $D^2\bar{R}$ is its acceleration relative to the rotating frame. The second term on the left hand side of Equation 1 is the Coriolis acceleration of P. \bar{F} is the external force per unit length experienced by the yarn.

These generalized equations of motion Equation 1 can now be used with appropriate modifications and boundary conditions to describe the physics of a particular problem. The external force, \bar{F} , can be understood more fully by looking at two cases without loss of generality.

Force Due to Air Drag on the Balloon

In case of a free balloon in air the vector \bar{F} is the force per unit length acting on the yarn due to air drag. Each

1. Padfield, D. G., 1955, J. Text. Inst. 46, T71-T77 and 1956, J. Text. Inst. 47, T301-T308.

2. Kothari, V. K., & Leaf, G. A. V., 1979, J. Text. Inst. 70, 89-95 and 95-105.

material element of the yarn can be considered a cylinder with its axis at an oblique angle to the air flow direction. Thus it is necessary to consider components of the air drag force in directions normal and tangential to the yarn. Earlier investigations have shown that the tangential component has relatively negligible effect on balloon shape and tension compared with the effect of the normal component. In the present investigation only the normal component of air drag has been considered.

The magnitude of the normal component on a circular cylinder is,

$$|F| = \frac{1}{2} C_D \rho d v_n^2 \quad (2)$$

where ρ ($=1.22 \text{ kg m}^{-3}$) is density of air, d is the effective diameter of the yarn, v_n is magnitude of the normal component of yarn velocity and C_D is the air drag coefficient. Finally, the air drag force acts in the direction $-v_n$, so that

$$\bar{v}_n = \frac{\partial \bar{R}}{\partial s} \wedge (\bar{v} \wedge \frac{\partial \bar{R}}{\partial s})$$

and

$$\bar{v} = D\bar{R} + \Omega \mathbf{k} \wedge \bar{R}$$

Force due to Frictional Drag on the Package Surface

The force acting on the yarn, while it slides over the package surface, as in unwinding is due to friction and pressure between moving yarn and the package. The magnitude of this frictional force, F , is assumed to be proportional to the normal force between the yarn and the package (Amonton's law) and it acts in the direction opposite to that of

motion. Thus $\bar{F} = -\mu \bar{N} \frac{\bar{v}}{|\bar{v}|} + \bar{N} \mathbf{e}_r$

where μ is the coefficient of yarn package frictional drag, N is the normal force per unit length between yarn and the package and v is the velocity of the yarn element.

On Unwinding of Yarn from a Cylindrical Package

The governing equations developed earlier can now be applied to analyze the problem of unwinding. Figure 2 shows a schematic of the yarn package and guide eye placed along the package axis. Our objective is to give a complete analysis of the yarn dynamics between the point where the yarn first starts moving away from its stationary position on the package surface (called the unwind point, U in Figure 2) and the guide eye. The motion is in two parts: the yarn first slides across the package surface until it lifts off and flies into the balloon. The point where that occurs is called the lift-off point (L in Figure 2). The time derivatives in the governing equations can be removed using the Perturbation theory, provided that wind angle is fairly small. A detailed discussion of the perturbation analysis is beyond the scope of this report, however, a brief account of the analysis follows. In perturbation analysis all variables are expanded in power series of the perturbation parameter ϵ , e.g.

$$R(s, t) = R_0(s, t) + \epsilon R_1(s, t) + \epsilon^2 R_2(s, t) + \dots \quad (3)$$

These expressions are substituted into the equations of motion and boundary conditions. Subsequently like powers of ϵ on both sides are equated to yield a hierarchy of equations from which the coefficient functions in the power series can be calculated. The parameter ϵ can be estimated from the withdrawal speed V , the wind angle ϕ , and the package height H , as $\epsilon = (c/2H) \sin \phi$. Typical values range from 0.007 to 0.1. Thus it is small compared to other parameters of the problem. So the terms involving higher powers of ϵ can be neglected as a first approximation. The zero-th order approximation of the equation of motion yields;

$$\frac{\partial^2 R_0}{\partial s^2} - 2\mathbf{k} \wedge \frac{\partial R_0}{\partial s} + \mathbf{k} \wedge (\mathbf{k} \wedge R_0) = \frac{\partial}{\partial s} \left(T_0 \frac{\partial R_0}{\partial s} \right) + F_0$$

Boundary Conditions at the Guide-eye

Boundary conditions at the guide-eye which is at the origin of the coordinate system are, $R(s=0) = 0$, the height of the balloon, $z(s=0)=0$, and because of the rotational symmetry of the problem, polar angle $\theta(s=0) = 0$.

Boundary conditions at the lift-off point

All continuity conditions at $s=s_1^-$ and $s=s_1^+$ must be satisfied, and the yarn must be tangent to the package surface.

Boundary conditions at the unwind point

The yarn dragging on the surface of the package must be at an angle equal to the wind angle at this point. i.e., $d\theta/ds = \cos\phi$, where ϕ is the wind angle, usually less than 15° . Time dependence of the unwinding process is included in the analysis through movement of the unwind point and is described by, $dz_u/dt = \Phi_u$, where Φ_u is a function of the wind program.

Alternatively, the residual tension (T_{res}) in the yarn as it lies in the package can be included as a boundary condition at the unwind point as, $T_u = T_{res}$, where T_u is the tension in the yarn at the unwind point.

Ring Spinning

As in the case of 2-for-1 twisting, the only inertial term that need be included in the equation of motion is that due to centripetal acceleration. In terms of dimensionless variables the equation is:

$$\mathbf{k} \wedge (\mathbf{k} \wedge \mathbf{R}) = \frac{d}{ds} \left(\bar{T} \frac{d\bar{\mathbf{R}}}{ds} \right) + \bar{\mathbf{F}}$$

where

$$\bar{T} = T/m\omega^2 a^2, \bar{\mathbf{F}} = -p_0/16|\bar{v}_n|\bar{v}_n, \text{ and, } p_0 = 16D_n a/m$$

Boundary Conditions at the Guide Eye

The boundary conditions are, radius of the balloon, $R(s=0) = 0$, height of the balloon, $z(s=0)=0$, and because of rotational symmetry, polar angle $\theta(s=0) = 0$.

Boundary Conditions at the Traveler

Let h be height of the guide eye above the ring and $s=s_1$ be length of yarn in the balloon. Thus the geometrical boundary conditions at the traveller are: radius of yarn balloon at the traveller, $r(s_1) = a$, and position of traveller along Z axis, $z(s_1) = h$. The other very important boundary condition is obtained from equation of motion of the traveller.

Without formal proof here, it can be shown that the yarn tension on the balloon side of the traveller is related to the traveller mass m_T , ring-traveller coefficient of friction, μ_T , and other geometrical parameters, as;

$$T_1 [g \sin\phi - a\theta'(s_1)] = \mu_T \sqrt{\{T_1 [r'(s_1) + g \cos\phi] - m_T \omega^2 a\}^2 + T_1^2 z'(s_1)^2}$$

The parameter $g = \exp(\mu_y \alpha)$, is traveller-yarn friction parameter, μ_y is coefficient of friction between yarn and traveller and α is the yarn angle of wrap around the traveller.

Results and Discussion

Numerical solutions of the boundary value problems(BVP) described in the last section have been obtained by using "shooting method." Details of this method can be found in publications by the PIs [1,2,3,5]. In the following we look at the highlights of the numerical results, obtained thus far, for each of the processes.

Unwinding of Cylindrical Packages

In unwinding, extensive computational studies have been carried out to understand the effects of changing wind-angle and "residual tension." It has been found that the balloon shape and tension distribution are critically determined by the "residual tension" in the yarn on the package just before it moves into sliding and the coefficient of yarn drag on the package. These results underline the importance of thread-line tension used in winding which eventually manifests as "soft" or "hard" package. To illustrate these results, a number of cases, defined in Table 1 will be discussed. Figure 3, illustrates the effect of wind angle on tension at the guide-eye. It is obvious that the calculated levels of tension are not significantly influenced by changing wind angle. In addition, Table 2 shows the non-unique-

ness of solutions obtained by specifying the wind angle as a boundary condition. The results show significantly different levels of guide eye tensions corresponding to a number of possible solutions for each case where wind angle is specified as a boundary condition. The multiple solutions (shape and tension) for case I with wind angle of 5 degrees are shown in Figure 4. Each solution in Table 2 corresponds to a calculated value of residual tension, suggesting uniqueness of solution if residual solution is specified as a boundary condition. In the subsequent calculations the BVP is modified to use the residual tension at the unwind point as a boundary condition instead of the wind angle. Calculated tension values, using the modified method, are presented in Table 3. The results show that for a given value of residual tension there is only one solution corresponding to the guide eye tension.

These theoretical investigations are continuing while experiments are being set up to develop a means of studying the residual tension as well as shape and tension distribution in the yarn balloon.

Table 1: Unwinding Parameters

	Radius of Package (mm)	Mass Linear Density of Yarn (denier)	Unwinding Velocity (m/min)	Balloon Height (mm.)	Package to Yarn Drag-Coefficient
Case I	42.5	112.5	500	255	0.4
Case II	85.0	112.5	1000	512	0.4
Case III	128	112.5	1000	768	0.4

Table 2: Non-uniqueness of Solution with Wind Angle as a Boundary Condition

	Case I		Case II		Case III	
Calculated T_0 (non-dimensional)	7.15	4.26	5.65	3.20	5.16	2.83
Calculated T_u (non-dimensional)	5.87	3.50	4.35	2.42	3.83	2.04

Table 3: Effect of Residual Tension on Guide-eye Tension

	Case I	Case II	Case III
Residual Tension, T_u , specified as a boundary condition	7.0	7.0	7.0
Calculated tension at the guide-eye, T_0	7.73	7.49	7.57

Ring Spinning

The models of ring spinning and related results, at the start of this project, are detailed in [1,2,4]. Fraser in an independent analysis [5] confirmed the results obtained in [1,2] but went on to show the existence of bifurcation phenomenon in ring spinning. In the non-dimensional parametric space, keeping all else constant, he studied the effect of variable traveler mass on the spinning tension and showed that for balloon height to ring radius ratio of ten, the spinning tension as well as balloon shape could have as many as three plausible (satisfying dynamic equilibrium) values provided the traveler mass was within a specified range. While this was an important conceptual finding, technologically it was meaningless because during spinning the traveler mass remains fixed whereas wind radius and balloon height change. To investigate practical implications of this issue, the NCSU team first enhanced their model to (a) calculate the wrap angle (yarn around the traveler) internally using equilibrium shapes of the balloon before and after yarn enters the traveler and (b) to include the chase formation program so that, having selected a height of top of the chase, the balloon height could be adjusted automatically for changing wind radius.

The practical implication of bifurcation can be explained through meta-stability of shape and tension. In other

words meta-stability here implies the possibility of rapid and wide spinning tension fluctuations with the likelihood of high rate of ends down. Therefore the present focus of this research is to map precisely the domains of this meta-stability within the practical range of interest. A plot of spinning tension with varying bobbin radius and balloon height is shown in Figure 5 for a typical ring-spinning set up without control rings. Projection of the outer limit of instability in the bobbin radius-balloon height plane is shown in Figure 6. It was shown earlier that placement of a control ring of suitable size at a suitable height could eliminate the meta-stability. Therefore, spinning without control rings must be avoided in these regions.

Experimental Set-up

The experimental part of the research is designed to verify the theoretical unwinding response predictions. Due to the complexity of the process being studied, four different experimental systems are planned. Two experiments, dealing with verifying the unwinding dynamics, have been initiated. Another two experiments determine the residual tension and yarn-package drag. These experiments are being designed.

The first experiment is based on an unwinding tester donated by Reiter-Scragg (PPA-2). In this system, packages of variable height, shape, wind angle, and wind-on tension can be unwound and the real-time tension variations recorded. In this research, we tap directly into the tension sensor to measure the real-time signal. Figure 7 shows the frequency spectrum of a cylindrical package. Peaks are observed at the rotation, longitudinal, and sensor resonant frequencies.

For a given yarn, package, and unwind speed, the tension time history and balloon shapes can be recorded. Quasi-stationary balloon shapes can be captured with the digital camera and compared with theory. Combined with the measured tension values, yarn on package drag, and residual tension, this experiment will verify the complete model. In addition, the dynamical complexity of this system will necessitate the use of a high speed video system to observe the transient motion caused by package irregularities.

The second experiment is designed to verify the balloon dynamics equations including air drag. The spinning experiment uses a hollow spindle motor threaded with a weighted string. The spindle spins the yarn without twist buildup and the tension and motor speed are monitored. A motorized arm varies the balloon height. Thus for a given yarn, tension, balloon height, and spindle speed, stable balloon shapes can be observed. Figure 8 shows the experimentally determined motor voltage, speed, and tension time histories when the balloon height is varied sinusoidally. Qualitative determination of the balloon shape can also be determined by photographs of the operating system.

The spinning experiment will be improved with a new spindle, spindle motor, and tension sensor. These design changes will allow higher spindle speeds and higher bandwidth tension measurements. Reiter-Scragg will be donating the tension sensor. In addition, we plan to purchase a digital camera to capture the balloon shapes for quantitative comparisons with theory.

In summary, two experiments have been partially constructed so far in this research program. The spinning experiment provides reliable, low speed, low bandwidth tension data. The system also produces stable, quasi-stationary balloons for theoretical comparisons. The PPA2 yarn transport and tension measurement systems provide an excellent test-bed for complete verification of the theory. The planned modifications to these systems will allow qualitative comparisons by the end of Year 3.

References: (Papers Published, in Preparation or Submitted since the start of the project)

1. Batra, Subhash K., Ghosh, Tushar K., and Zeidman, Mishu I., An Integrated Approach to Dynamic Analysis of the Ring Spinning Process, Part I: Without Air Drag and Coriolis Acceleration, *Textile Research Journal* 59(6), 309-317 (1989).
2. Batra, Subhash K., Ghosh, Tushar K., and Zeidman, Mishu I., An Integrated Approach to Dynamic Analysis of the Ring Spinning Process, Part II: With Air Drag, *Textile Research Journal* 59(7), 416-424 (1989).
3. W. B. Fraser, T. K. Ghosh, S. K. Batra, "On unwinding yarn from a cylindrical package," *Proc. R. Soc. Lond.* (1992) 436, 479-498;
4. T. K. Ghosh, S. K. Batra, M. I. Zeidman, B. Dua, "An Integrated Approach to Dynamic Analysis of the Ring Spinning Process, Part III. The Effect of Coefficient of Friction and the Balloon Control Rings," *Textile Praxis International*, (in English and German) September 1992.
5. W. B. Fraser, "On the Theory of Ring Spinning," *Phil. Trans. R. Soc. Lond.* vol. 342, pp439-468, 1993 (Part IV)
6. S. K. Batra, T. K. Ghosh, W. B. Fraser, K. Q. Robert Jr. "An Integrated Approach to Dynamic Analysis of the Ring Spinning Process, Part V. Inherent Instability of the Free Balloon," *Proc. R. Soc. Lond.* (submitted)

7. W. B. Fraser, "Effect of Yarn Elasticity On an Unwinding Balloon," J. Text. Inst., vol 83, pp603--613, 1992.
8. W. B. Fraser, "On the Dynamics of Two-for-One Twister," Proc. Royal Soc. London, Ser. A, (in press) 1993.
9. W. B. Fraser, "Air-drag and Friction in the Two-for-One Twister: results from the theory," J. Text. Inst. (in press), 1993.
10. W. B. Fraser, S. K. Batra, T. K. Ghosh, "On the Dynamics of Yarn Ballooning," Invited paper at the Gordon Research Conference on Fiber Science, New London, NH, July 11-16(1993)

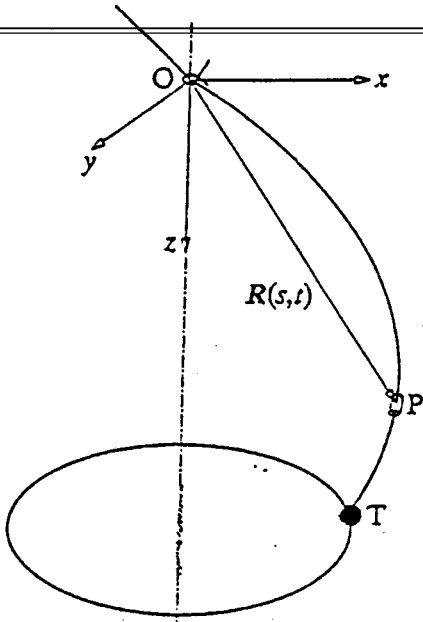


Fig 1. The thread line

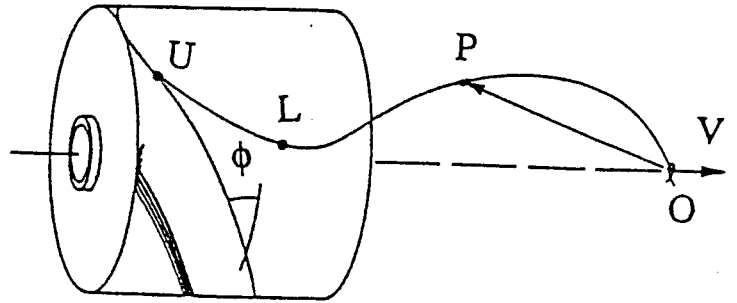


Fig 2. Over-end uninding configuration : guide eye O; balloon OPL; lift-off point L; unwind point U ; wind-on angle ϕ ; withdrawal speed V;

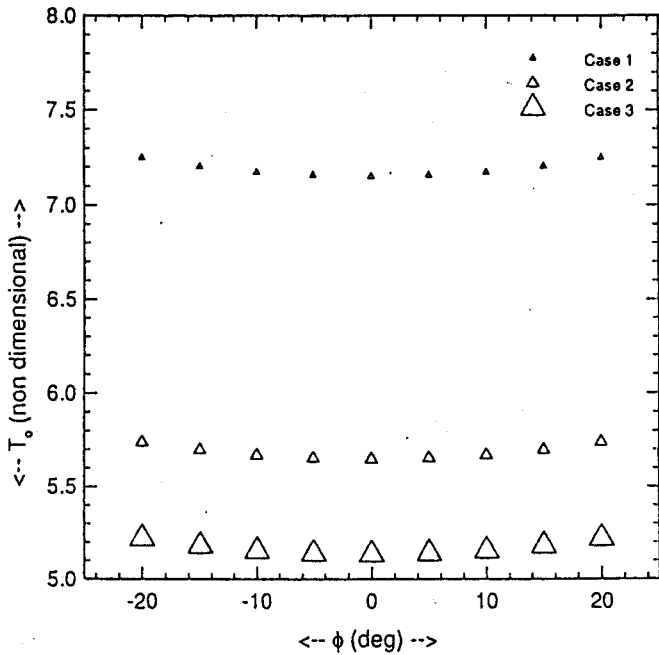


Figure 3. Effect of wind angle on tension at the guide-eye

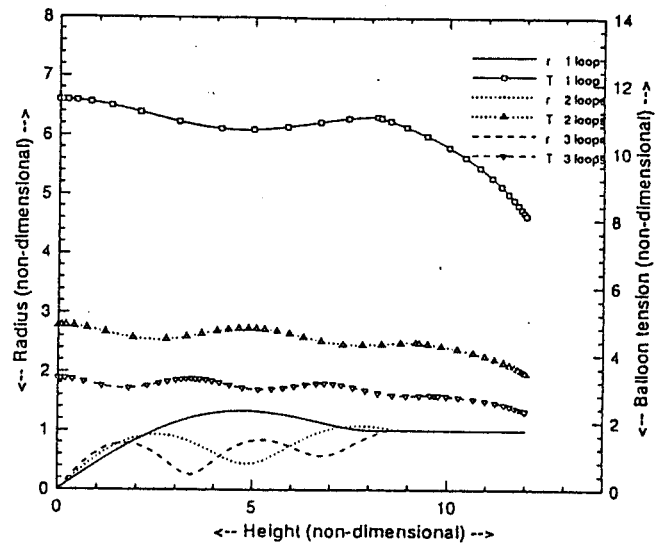


Figure 4. Multiple solutions (shape and tension) for Case I with wind angle of 5 degrees

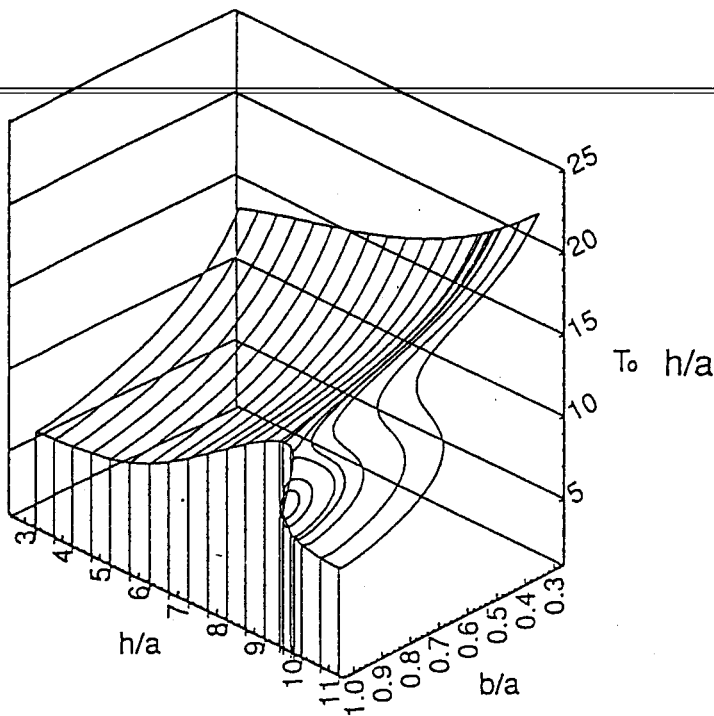


Figure 5. A plot of spinning tension with varying bobbin radius and balloon height ($TM=90.0, m_y=0.3, \mu_y=0.1, P_0=3.0$)

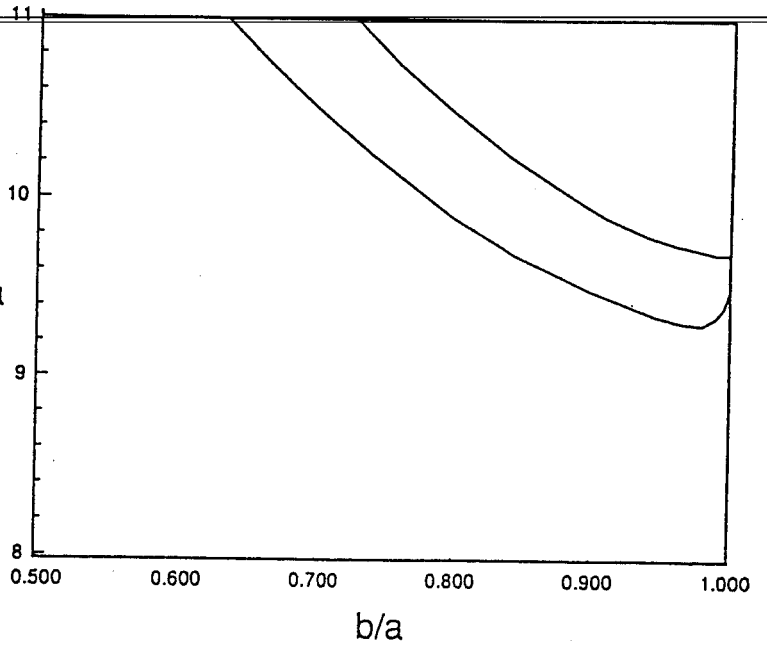


Figure 6. Projection of the outer limit of instability in the bobbin radius and balloon-height plane ($TM=90.0, \mu_y=0.3, \mu_y=0.1, P_0=3.0$)

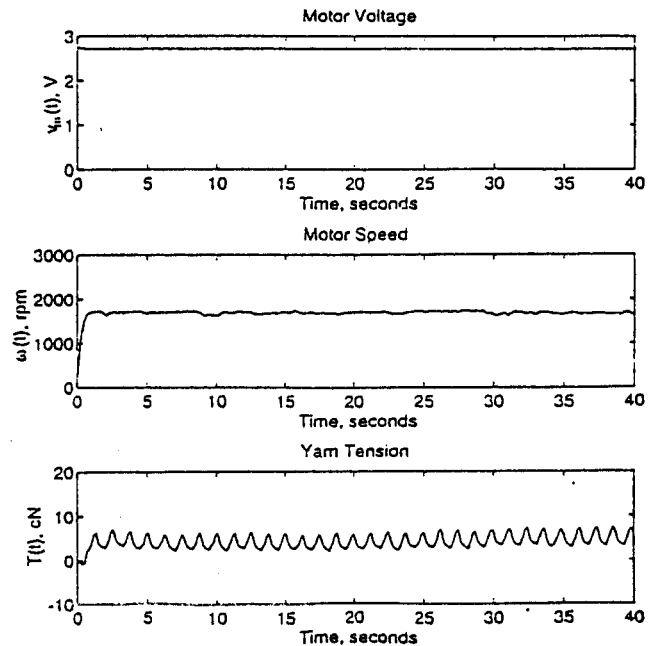
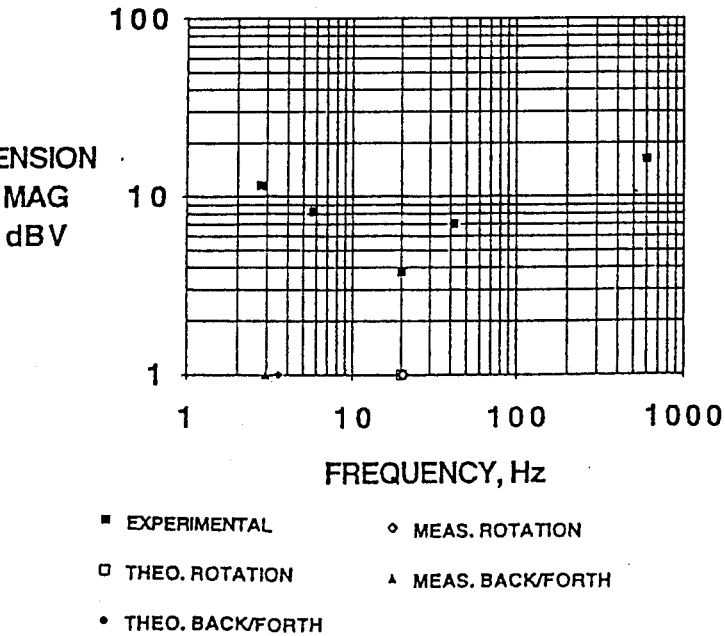


Figure 7. Tension frequency spectrum of a cylindrical package

Figure 8. Experimentally determined motor voltage, speed, and tension-time histories when the balloon height is varied sinusoidally

